AGH University of Science and Technology
Krakow, Poland

SANi South African Nanotechnology Initiative
Research & Higher Degrees
NanoAfrica 2014
5th International Conference on Nanoscience & Nanotechnology
Vaal University of Technology, Department of Chemistry
Science Park—Sedibeng Campus—Vanderbijlpark
30 March—02 April 2014
VUT Vaal University of Technology

New precursor route to nanocrystalline powders of magnetic manganese nitride η-Mn$_3$N$_2$

<u>Jerzy F. Janik</u>[1a], Mariusz Drygas[1a], Michal Musial[1a#],
Miroslaw M. Bucko[1b], Jacek Gosk[2], Andrzej Twardowski[2]

[1] *AGH University of Science and Technology,* [a]*Faculty of Energy and Fuels,* [a#]*graduate student,*
[b] *Faculty of Materials Science and Ceramics; al. Mickiewicza 30, 30-059 Krakow, Poland;*
[2] *University of Warsaw, Faculty of Physics, Institute of Experimental Physics, ul. Hoza 69,*
*00-681 Warsaw, Poland*

SPINTRONICS or SPIN TRansport electrONICS
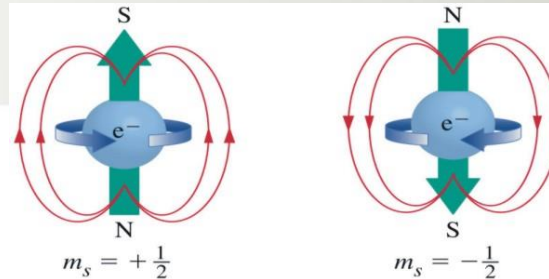
Electronics: the charge of electrons is utilized in most of contemporary electronic devices.

Spintronics: the spin of electrons is controlled in addition to or, sometimes, in place of the charge of electrons.

Spintronics in semiconductors - spin based electronics takes on adding the spin (magnetism) to already exploited charge of the electron (electronics) to carry information (transport) which means that the utilization of both semiconducting and magnetic properties residing in one otherwise „homogeneous" material is anticipated.
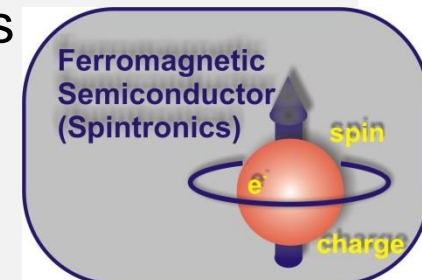
Where do we come from?
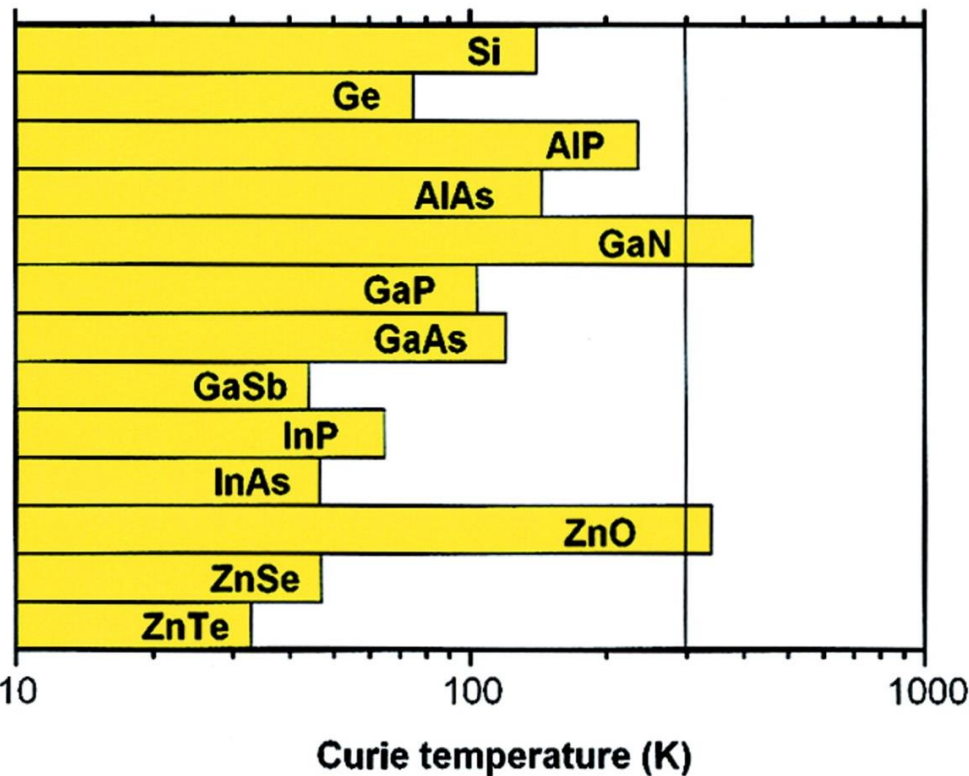
Computed values of the Curie temperature T_C for various p-type semiconductors containing 5 % of Mn and 3.5×10^{20} holes per cm^3.

(T. Dietl, H. Ohno, F. Matsukura, J. Cibert, D. Ferrand; *Science* **2000**, vol. 287, No. 5455, 1019)

Since 2000, numerous attempts for thin films prepared by various deposition technigues and for mono- and microcrystals have failed to demonstrate RT ferromagnetism in the GaN/Mn system.

Nanomaterials with up to 2 wt% incorporated Mn were prepared in our group with the convenient aerosol-assisted method utilizing commercially available metal precursors as well as *via* our anaerobic route utilizing the known gallium amide precursor $Ga[N(CH_3)_2]_3$.

(1. J. F. Janik, M. Drygas, C. Czosnek, M. Kaminska, M. Palczewska, R. T. Paine, *J. Phys. Chem. Solids*, **2004**, vol. 65, 639.
2. J. B. Gosk, M. Drygas, J. F. Janik, M. Palczewska, R. T. Paine, A. Twardowski, *J. Phys. D: Appl. Phys.,* **2006**, vol. 39, 3717)

How about Mn^{3+}:

- in nanocrystalline powders of GaN?
- on surfaces of GaN nanoparticles?
- under sintering conditions of GaN/Mn nanopowders?

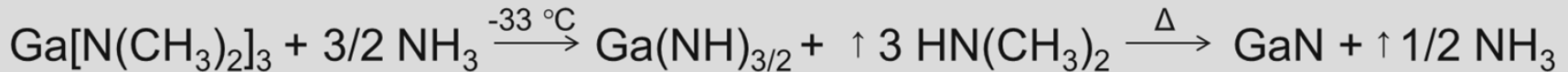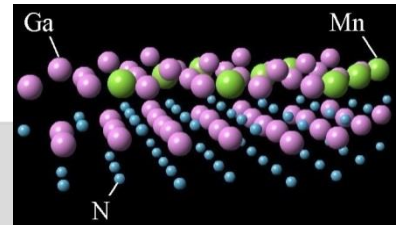Utilize aneaerobic synthesis method and oxyden-free gallium and manganese precursors to provide best synthetic conditions for the preparation of the target nanopowders, *i.e.,* both nanocrystalline (Ga,Mn)N substitutional DMS and (Ga,Mn)N / Mn multiphase materials.

These nanopowder are further planned to be processed *via* high-pressure high-temperature powder sintering as well as surface functionalization towards advantageous magnetic phases.
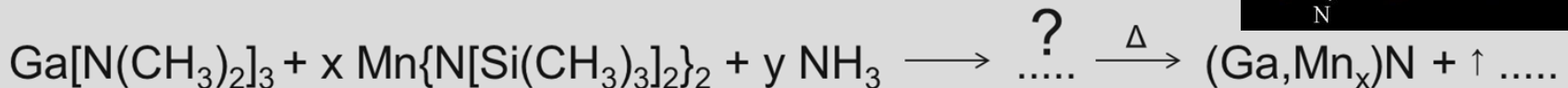
What we know: (J. F. Janik, R. L. Wells, *Chem. Mater.* **1996**, vol. 8, 2708)
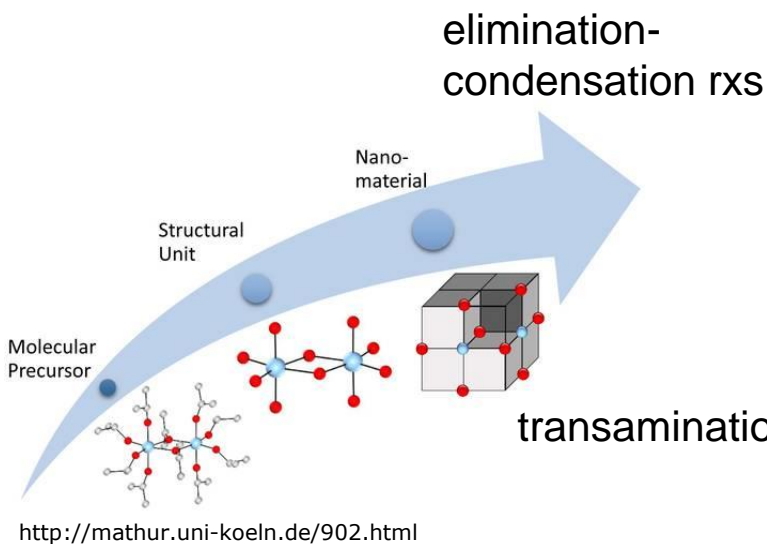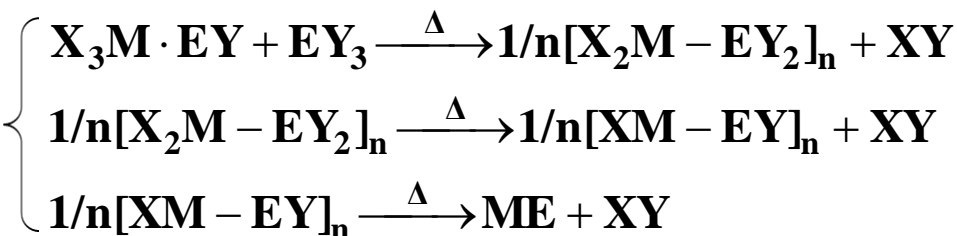
$$Ga[N(CH_3)_2]_3 + 3/2\ NH_3 \xrightarrow{-33\ °C} Ga(NH)_{3/2} + \uparrow 3\ HN(CH_3)_2 \xrightarrow{\Delta} GaN + \uparrow 1/2\ NH_3$$

http://www.sciencedaily.com/releases/2013/06/130606112036.htm

What we aim at:

$$Ga[N(CH_3)_2]_3 + x\ Mn\{N[Si(CH_3)_3]_2\}_2 + y\ NH_3 \longrightarrow \underset{.....}{?} \xrightarrow{\Delta} (Ga,Mn_x)N + \uparrow .....$$

Chemistry of materials precursors – bottom-up way to nanocrystalline materials

1:1 stoichiometry of M (Group III) to E (Group V); X, Y – ligands; XY – small, volatile molecule
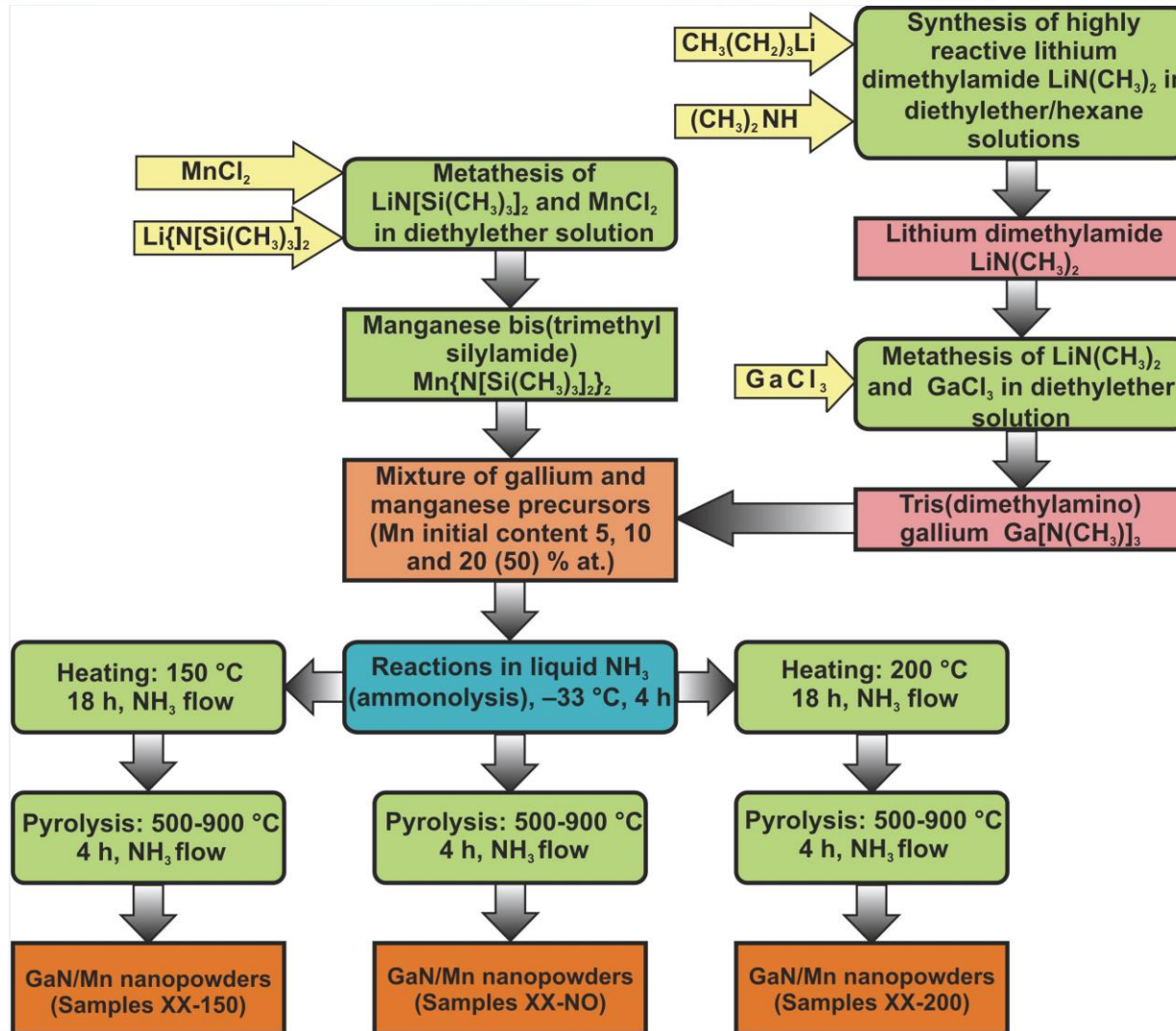
$$MX_3 + EY_3 \longrightarrow X_3M \cdot EY_3; \quad \text{Lewis adduct}$$

elimination-condensation rxs

$$X_3M \cdot EY + EY_3 \xrightarrow{\Delta} 1/n[X_2M - EY_2]_n + XY$$

$$1/n[X_2M - EY_2]_n \xrightarrow{\Delta} 1/n[XM - EY]_n + XY$$

$$1/n[XM - EY]_n \xrightarrow{\Delta} ME + XY$$

Δ - temperature-driven reactions

For nanonitrides: excess of E = N; R = organic ligand

transamination

$$M(NR_2)_3 + 3NH_3 \longrightarrow M(NH_2)_3 + 3HNR_2$$

deamination rxs

$$M(NH_2)_3 \xrightarrow{\Delta} 1/n[M(NH_2)(NH)]_n + NH_3$$

$$1/n[M(NH_2)(NH)]_n \xrightarrow{\Delta} 1/n[M(NH)_{3/2}]_n + 1/2NH_3$$

$$1/n[M(NH)_{3/2}]_n \xrightarrow{\Delta} MN + 1/2NH_3$$

Nano-material

Structural Unit

Molecular Precursor

http://mathur.uni-koeln.de/902.html
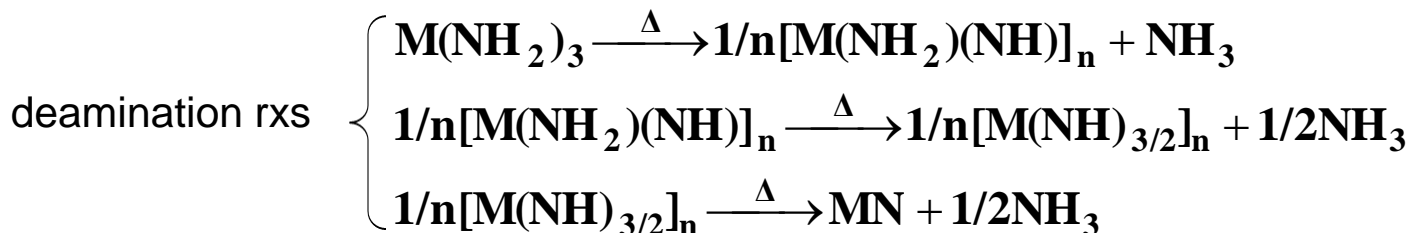
Chemistry of materials precursors in the making…

Niewa, R.: Nitridocompounds of manganese: manganese nitrides and nitridomanganates. Z. Kristallogr. **217** (2002) 8-23.

Binary phases in the system Mn−N: bond lengths d(Mn−N) and crystallographic data.

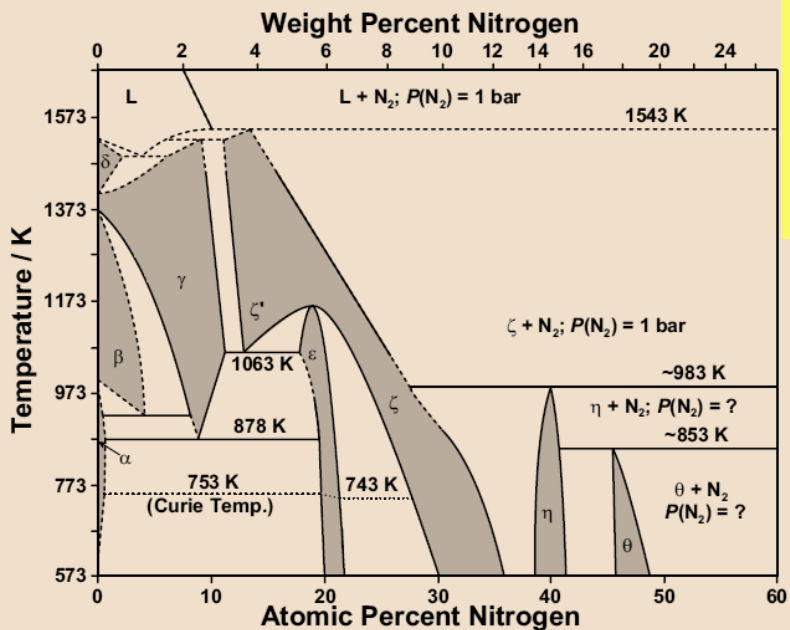| Phase	Composition	CN(Mn)	d(Mn−N) [pm]	Space group	Unit cell parameters [pm]
ε-Mn$_4$N	Mn$_4$N	2 (12)	2×192.9	$Pm3m$	$a = 386.8$
ζ-Mn$_2$N	Mn$_2$N$_{0.86}$	6	6×197.6^a	$P6_322$	$a = 489.16$
					$c = 455.45$
	Mn$_2$N$_{0.98}$	3	1×199.0	$Pbna$	$a = 566.8$
			2×199.2		$b = 490.9$
					$c = 453.7$
η-Mn$_3$N$_2$	Mn$_3$N$_2$	2, 5	$2 \times 193.2(6)$	$F4/mmm^b$	$a = 420.6(1)$
			$\mathbf{4 \times 210.5(4)}$	($I4/mmm$)	$c = 1212.6(4)$
			$\mathbf{1 \times 211.1(6)}$		
θ-Mn$_6$N$_5$	Mn$_6$N$_{5.26}$	6	$2 \times 206.44(1)^a$	$F4/mmm$	$a = 421.93(1)$
			$4 \times 210.97(1)^a$	($I4/mmm$)	$c = 412.87(1)$

a: N sites not fully occupied.
b: The crystallographic I-centered unit cell is obtained with $d' = a/\sqrt{2}$

Gokcen, N. A.: The Mn−N (Manganese-Nitrogen) System. Bull. Alloy Phase Diagrams **11** (1990) 33−42.

Results of the X-ray diffraction measurements for the MnN compound annealed in vacuum for 2 h at various temperatures

Annealing temperature (K)	Phase analysis
673	θ (MnN)
713	θ (MnN)
738	θ (MnN)
753	θ (MnN)
758	η (Mn$_3$N$_2$)
800	η (Mn$_3$N$_2$)
843	η (Mn$_3$N$_2$)
848	η (Mn$_3$N$_2$)+ζ
893	η (Mn$_3$N$_2$)+ζ
898	ζ
933	ζ
978	ζ
983	ζ+ε (Mn$_4$N)
1033	ε (Mn$_4$N)+ζ
1063	ε (Mn$_4$N)+ζ
1068	ε (Mn$_4$N)
1133	ε (Mn$_4$N)
1183	ε (Mn$_4$N)

Suzuki, K.; Kaneko, T.; Yoshida, H.; Obi, Y.; Fujimori, H.; Morita, H.: Crystal structure and magnetic properties of the compound MnN. J. Alloys Comp. **306** (2000) 66−71.

Tetragonal face-centered θ-MnN
– antiferromagnetic
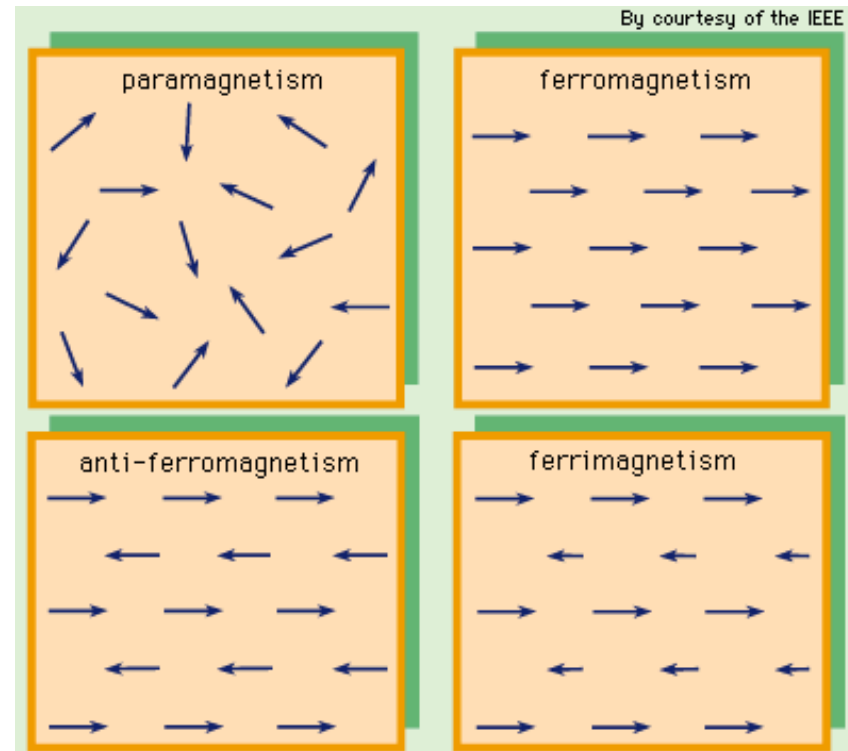(antiferromagnetic along [001] direction while ferromagnetic within (001) layer)

Tetragonal face-centered η-Mn$_3$N$_2$
– antiferromagnetic

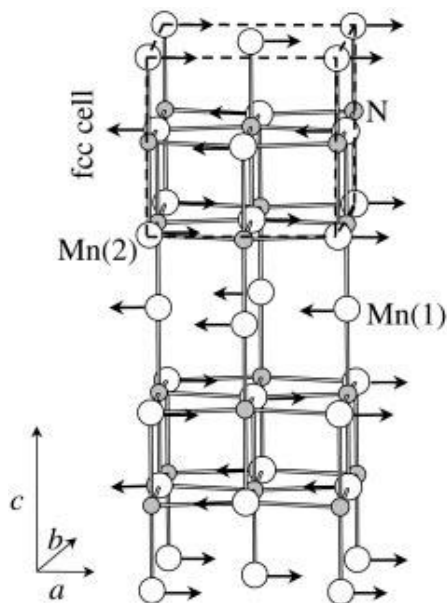Hexagonal closed-packed ζ-Mn$_5$N$_2$, Mn$_2$N – antiferromagnetic

Cubic face-centered ε-Mn$_4$N
– ferrimagnetic

By courtesy of the IEEE

paramagnetism ferromagnetism

anti-ferromagnetism ferrimagnetism

Nuclear and spin structure of η-Mn$_3$N$_2$ given for one unit cell in a face-centered tetragonal setting. The arrows represent the magnetic moments according to the antiferromagnetic structure of the first kind. The dashed lines indicate the pseudo-cubic unit cell of the rocksalt type.

Leineweber, A.; Niewa, R.; Jacobs, H.; Kockelmann, W. *J. Mater. Chem.* **2000**, *10*, 2827

η-Mn$_3$N$_2$ θ-Mn$_6$N$_5$
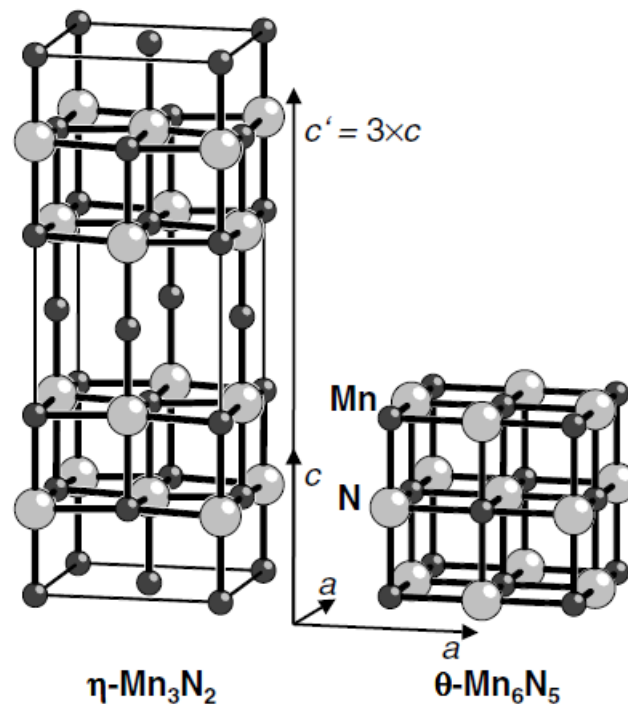
Comparison of the tetragonal unit cells of η-Mn$_3$N$_2$ (left) and θ-Mn$_6$N$_5$ (right) in the F-centered setting. While in the θ-phase, the nitrogen site is not fully occupied, the order in the nitrogen substructure of η-Mn$_3$N$_2$ leads to two distinct sites for manganese: one two-fold coordinated and one surrounded by a square pyramid, and to a three times enlarged unit cell parameter c.

Niewa, R. *Z. Kristallogr.* **2002**, *217*, 8

Previous work on synthesis of manganese nitrides

✓ Nitridation of Mn-powder with ammonia NH_3 (1945)

✓ Reactions od Mn-amalgams with N_2 or NH_3 (1894-1962)

✓ Preparation of thin films by nitridation of Mn-films with ammonia (1977)

✓ DC reactive sputtering in the system Mn / N_2 (1993)

✓ MBE-grown films in Mn / RF N-plasma (2005)

✓ High pressure synthesis in the system Mn / N_2, 10 GPa (2005)

✓ Microvawe synthesis in the system Mn / N_2 (2007)

✓ **Solvothermal metal azide decomposition to *nanocrystalline* Mn-nitrides (2009)**

Choi, J.; Gillan, E. G. Inorg. Chem. 2009, 48(10), 4470

⬇

HT-HP autoclave reactions in the system $MnCl_2$ / NaN_3 / toluene, 290 ºC

⬇

- tetragonal θ-MnN or a mixture of tetragonal η-Mn_3N_2 and cubic ε-Mn_4N
- av. crystallite sizes *ca.* 20 nm

Reaction conditions: A – 2 mmol $Mn[N(TMS)_2]_2$ in refluxing NH_3 at –33 ºC, 4 hrs; then, evaporation of NH_3 and an overnight evacuation of volatiles at RT

B – 1 mmol of $Mn[N(TMS)_2]_2$ and ammonia gas at RT, 1:4 mole ratio, 4 hrs; subsequently, 0.5 hr-evacuation of volatiles at RT
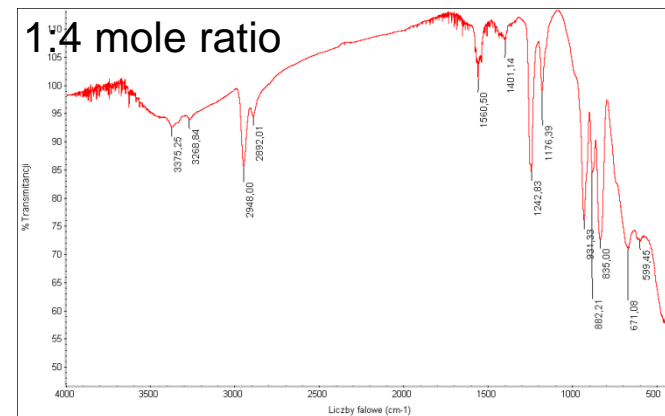
Product: light beige powders for A and B

Large excess of NH_3
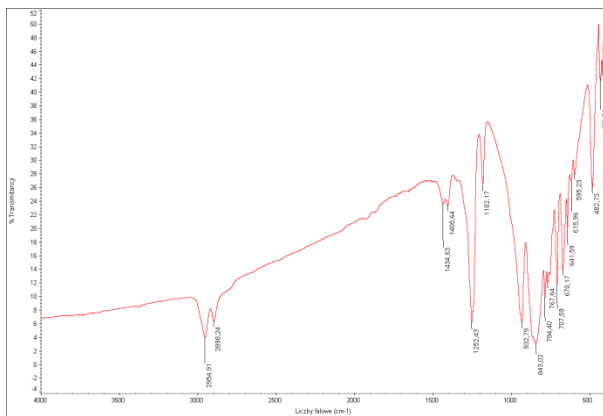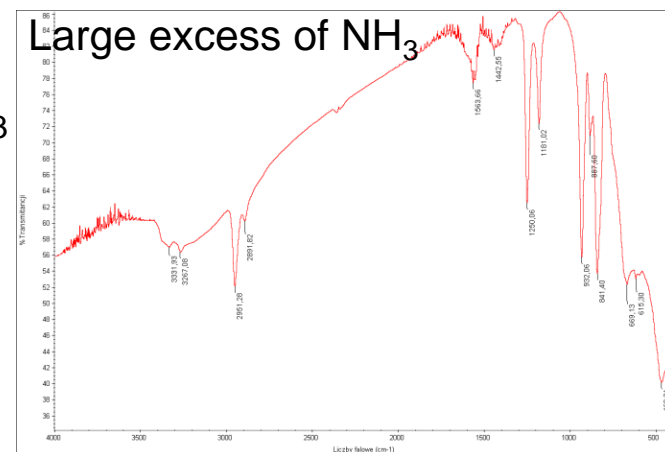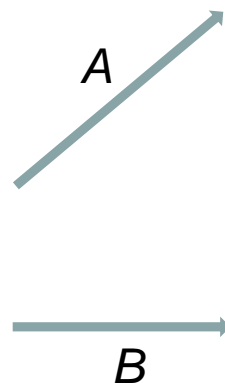
FT-IR spectrum of powder product from A

A

FT-IR spectrum of $Mn[N(TMS)_2]_2$

B

1:4 mole ratio

FT-IR spectrum of powder product from B

(i) The distinct bands at *ca.* 3250-3350 cm^{-1} superimposed on the broad feature at 3200-3500 cm^{-1} and the bands at *ca.* 1550-1600 cm^{-1} are typical for the stretching and deformation modes of N-H, respectively, in the –NH$_2$ and =NH groups.

(ii) In the volatiles from the exps. *A* and *B*, hexamethyldisilazane HN(TMS)$_2$ was detected by FT-IR which supports the transamination occurring in the system.

(iii) The solid products show some –TMS groups still present at RT in addition to the –NH$_2$ and =NH groups.

(iv) The products are insoluble in hexane or diethylether pointing to their polymeric nature.

Conclusion: **partial transamination and formation of Mn[N(TMS)$_2$]$_x$(NH$_2$)$_y$(NH)$_z$**

This study – reactions of Mn[N(TMS)$_2$]$_2$ with HN(CH$_3$)$_2$

Reaction conditions: *C* – 2 mmol Mn[N(TMS)$_2$]$_2$ reacted with large excess of liquid HN(CH$_3$)$_2$ at 0 °C, 0.5 hrs; then, evacuation of volatiles at RT for 1 hr.

D – 1 mmol of Mn[N(TMS)$_2$]$_2$ and HN(CH$_3$)$_2$ gas at RT, 1:4 mole ratio, 0.5 hrs; then, collecting the volatiles in a FT-IR gas cell.
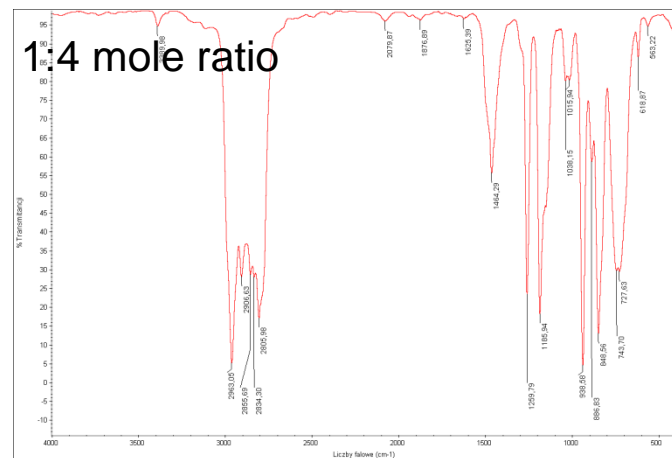
Product: grayish powder products for *C* and *D*

Large excess of amine

FT-IR spectrum of powder product from *C*

C

D

FT-IR spectrum of Mn[N(TMS)$_2$]$_2$

1:4 mole ratio
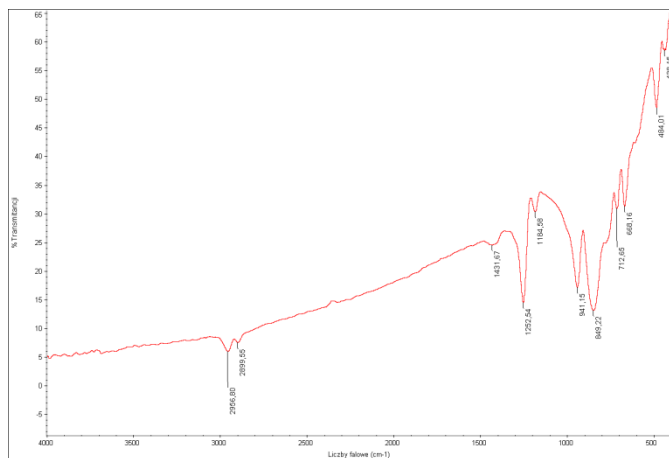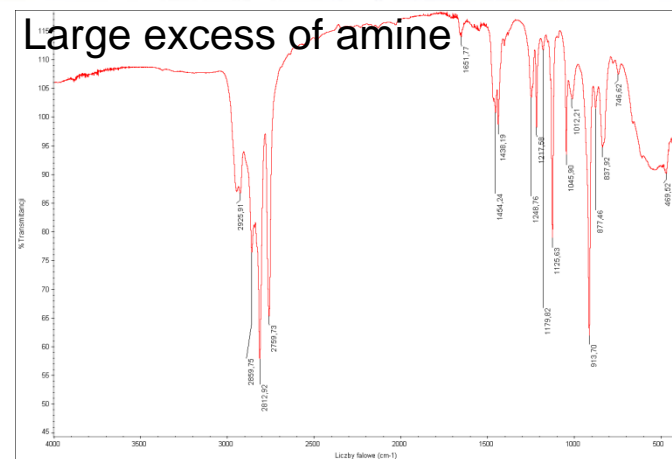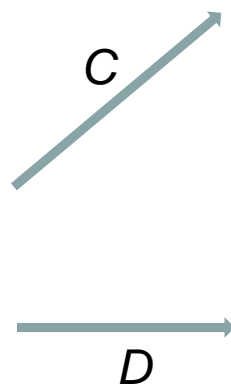
FT-IR spectrum of gases from exp. D

Reaction conditions: *C* – 2 mmol Mn[N(TMS)$_2$]$_2$ reacted with large excess of liquid HN(CH$_3$)$_2$ at 0 ºC, 0.5 hrs followed by evacuation of volatiles at RT for 1 hr.

E – powder product from *C* (above) reacted with large excees of refluxing NH$_3$ at –33 ºC, 4 hrs followed by evaporation of NH$_3$ and an overnight evacuation of volatiles at RT.

Product: grayish powder product for *E*
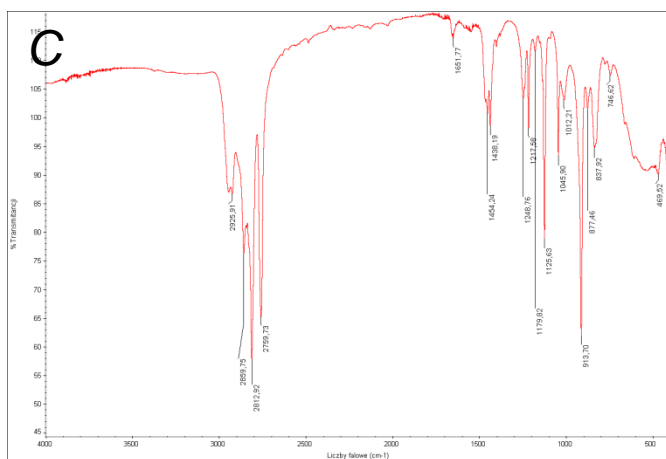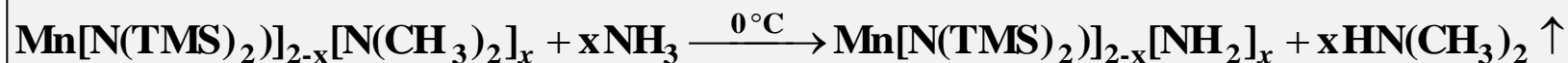

FT-IR spectrum of powder product from *C*

excess NH$_3$
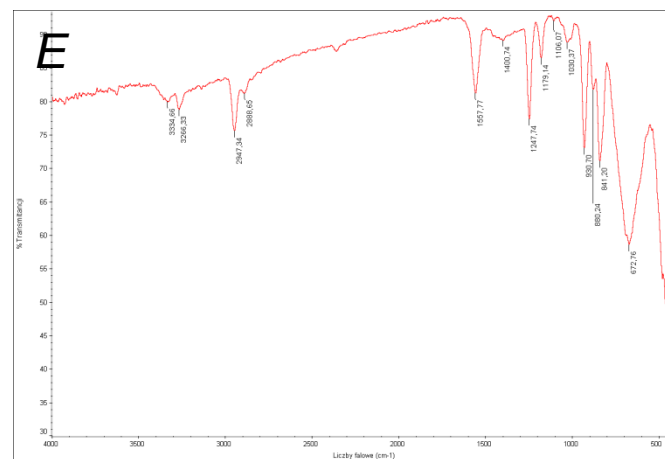
FT-IR spectrum of powder product from *E*

(i) In the volatiles from rx *D*, in addition to dimethylamine HN(CH$_3$)$_2$, hexamethyldisilazane HN(TMS)$_2$ was detected by IR which supports the transamination occurring in the system.

(ii) The solid product from rxs *C/D*, *i.e.*, Mn[N(TMS)$_2$]$_2$ + HN(CH$_3$)$_2$, shows some –TMS groups still present in addition to the dimethylamine groups supporting incomplete transamination.
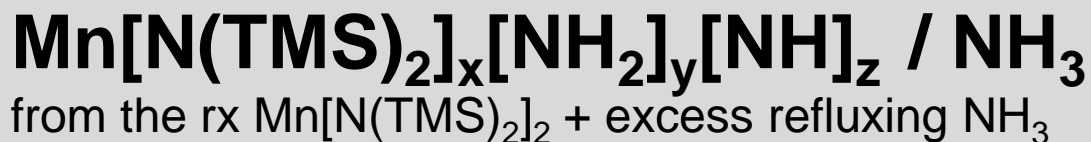
$$\text{Mn[N(TMS)}_2]_2 + x\,\text{HN(CH}_3)_2 \xrightarrow{0\,°C} \text{Mn[N(TMS)}_2)]_{2\text{-}x}[\text{N(CH}_3)_2]_x + x\,\text{HN(TMS)}_2 \uparrow$$

(iii) Product from rx *E (C* + excess NH$_3$) displays by IR similar characteristics as found for rxs *A/B* suggesting transamination/replacement of the –N(CH$_3$)$_2$ groups by, mostly, the –NH$_2$ groups; the latter is substantiated by the lack of the broad feature at *ca.* 3200-3500 cm^{-1} typical for plausible imide-type –(H)N– linkages in a polymeric/condensing network of Mn-N that could also be formed.
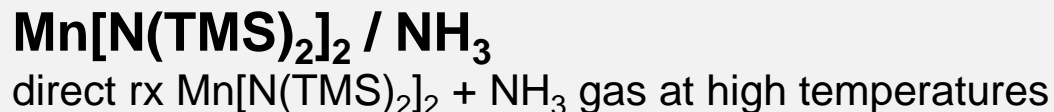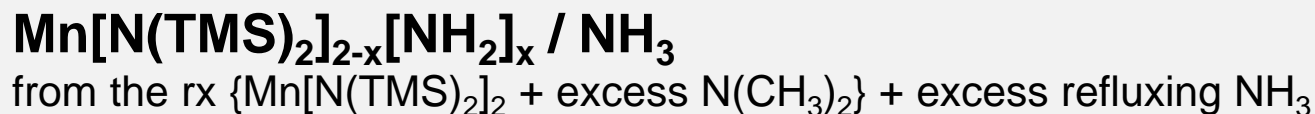
$$\text{Mn[N(TMS)}_2)]_{2\text{-}x}[\text{N(CH}_3)_2]_x + x\,\text{NH}_3 \xrightarrow{0\,°C} \text{Mn[N(TMS)}_2)]_{2\text{-}x}[\text{NH}_2]_x + x\,\text{HN(CH}_3)_2 \uparrow$$

AGH

Pyrolysis of the precursor under an ammonia flow at elevated temperatures in the range 150-900 ºC
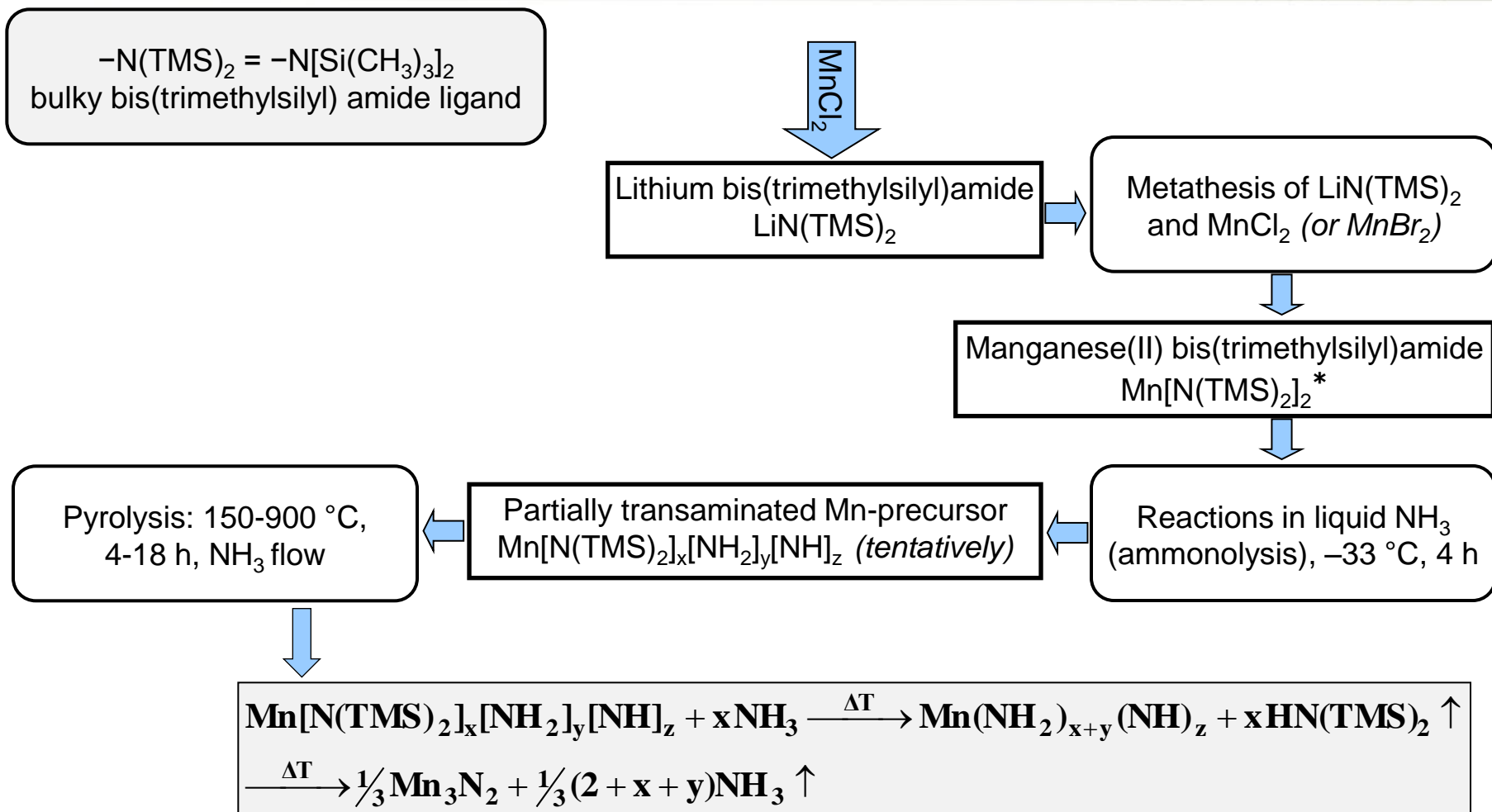
Current precursor system:

$Mn[N(TMS)_2]_x[NH_2]_y[NH]_z$ / NH_3
from the rx $Mn[N(TMS)_2]_2$ + excess refluxing NH_3

Other plausible precursor systems:

$Mn[N(TMS)_2]_{2-x}[NH_2]_x$ / NH_3
from the rx {$Mn[N(TMS)_2]_2$ + excess $N(CH_3)_2$} + excess refluxing NH_3

$Mn[N(TMS)_2]_2$ / NH_3
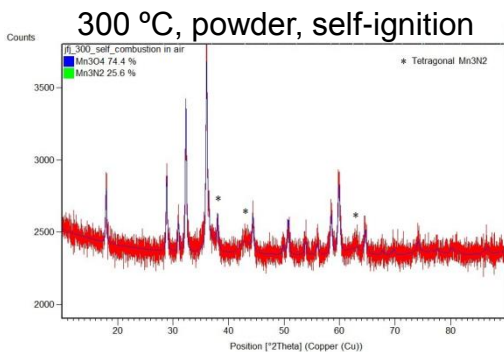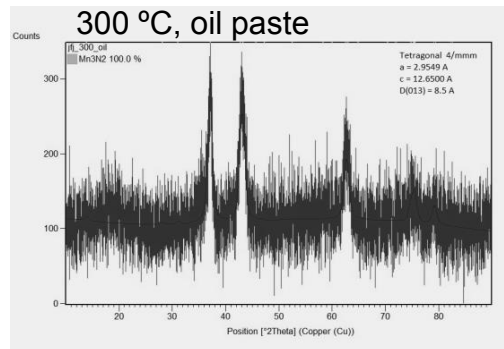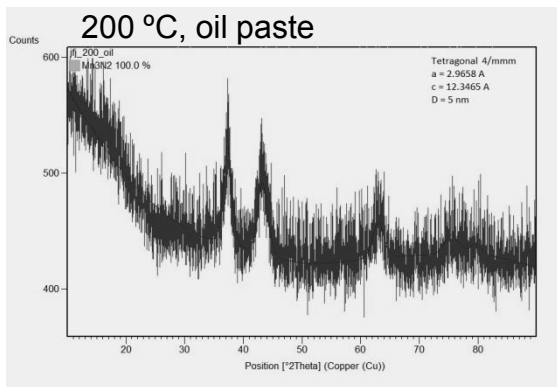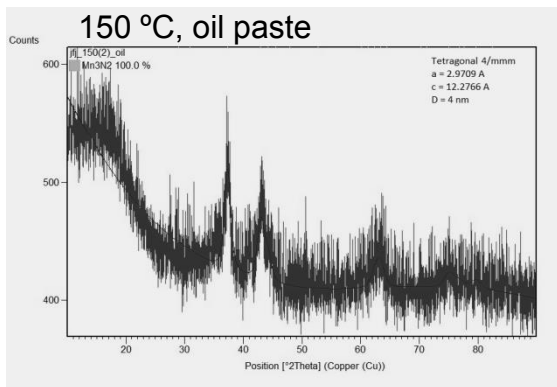direct rx $Mn[N(TMS)_2]_2$ + NH_3 gas at high temperatures

+
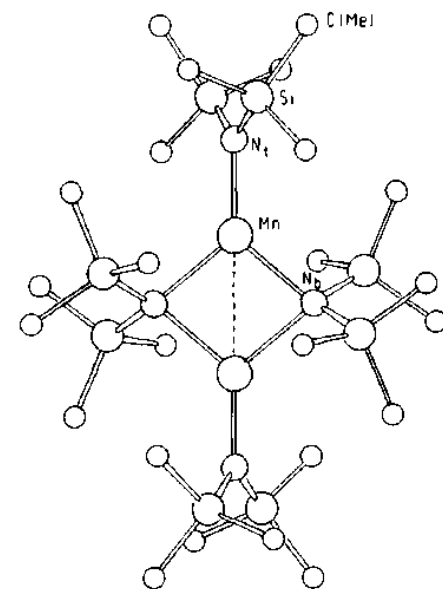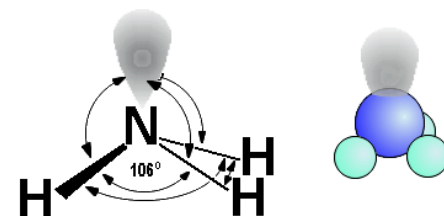
This work – anaerobic synthesis of Mn₃N₂ nanopowders

−N(TMS)$_2$ = −N[Si(CH$_3$)$_3$]$_2$
bulky bis(trimethylsilyl) amide ligand

MnCl$_2$

Lithium bis(trimethylsilyl)amide
LiN(TMS)$_2$

Metathesis of LiN(TMS)$_2$
and MnCl$_2$ *(or MnBr$_2$)*

Manganese(II) bis(trimethylsilyl)amide
Mn[N(TMS)$_2$]$_2$*

Pyrolysis: 150-900 °C,
4-18 h, NH$_3$ flow

Partially transaminated Mn-precursor
Mn[N(TMS)$_2$]$_x$[NH$_2$]$_y$[NH]$_z$ *(tentatively)*

Reactions in liquid NH$_3$
(ammonolysis), –33 °C, 4 h

$$Mn[N(TMS)_2]_x[NH_2]_y[NH]_z + xNH_3 \xrightarrow{\Delta T} Mn(NH_2)_{x+y}(NH)_z + xHN(TMS)_2 \uparrow$$

$$\xrightarrow{\Delta T} \tfrac{1}{3}Mn_3N_2 + \tfrac{1}{3}(2+x+y)NH_3 \uparrow$$

*Horvath, B.; Möseler, R.; Horvath, E. G. *Z. Anorg. Allg. Chem.* **450** (1979) 165-177.

Results -
# XRD diffraction patterns of powders and/or oil pastes

Product (pyrolysis conds, sample)	Crystallographic phase(s)	Lattice constants for η-Mn_3N_2 [Å]	Av. crystallite size of η-Mn_3N_2 [nm]
150 ºC, 18 hrs - oil paste	η-Mn_3N_2 tetragonal 4/mmm	a=2.97 c=12.28	4
200 ºC, 18 hrs - oil paste	η-Mn_3N_2 tetragonal 4/mmm	a=2.97 c=12.35	5
300 ºC, 4 hrs - oil paste	η-Mn_3N_2 tetragonal 4/mmm	a=2.95 c=12.65	8.5
300 ºC, 4 hrs - powder (self-ignition)	η-Mn_3N_2, 24 % Mn_3O_4, 76 %	n/d	n/d
500 ºC, 4 hrs - powder	η-Mn_3N_2, 62 % MnO, 38 %	a=2.98 c=12.45	25
700 ºC, 4 hrs - powder	η-Mn_3N_2, 54 % MnO, 46 %	a=2.98 c=12.42	76
700 ºC, 4 hrs - oil paste	η-Mn_3N_2, 98 % MnO, 2 %	a=2.99 c=12.45	95
900 ºC, 4 hrs - powder	η-Mn_3N_2 (I), 24 %	a=2.99 c=12.34	113
	η-Mn_3N_2 (II), 6 %	a=2.97 c=12.13	170
	MnO, 70 %		

Results - FT-IR determinations (KBr pellets)

Powder, 150 ºC, 20 hrs

Determination 1

Determination 2

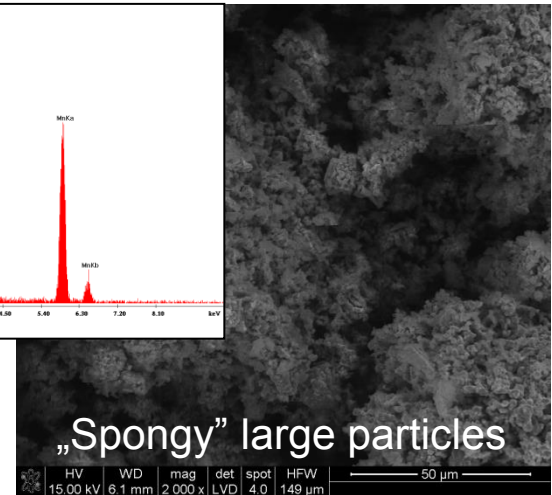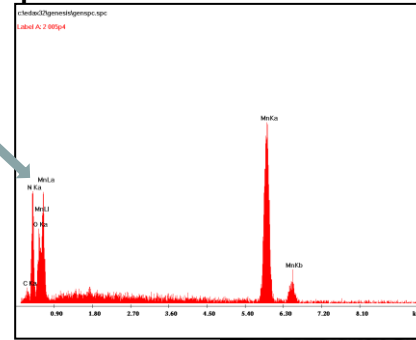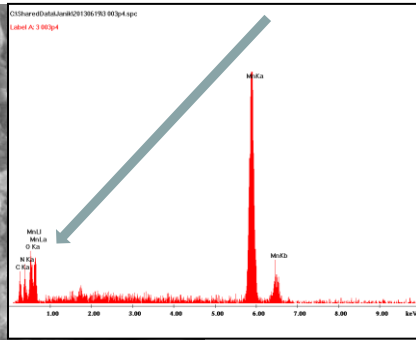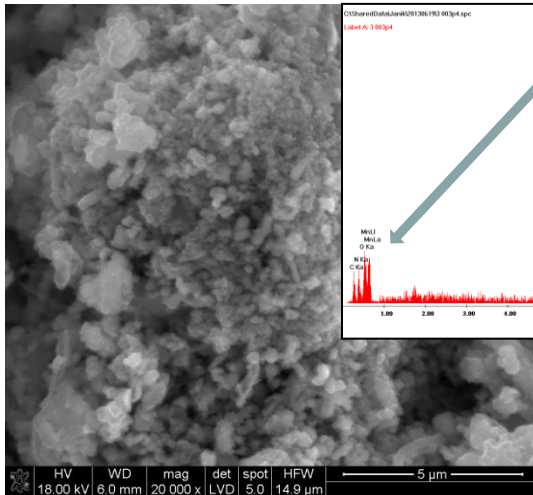## Powder, 700 ºC, 4 hrs

Determination 1

Determination 2
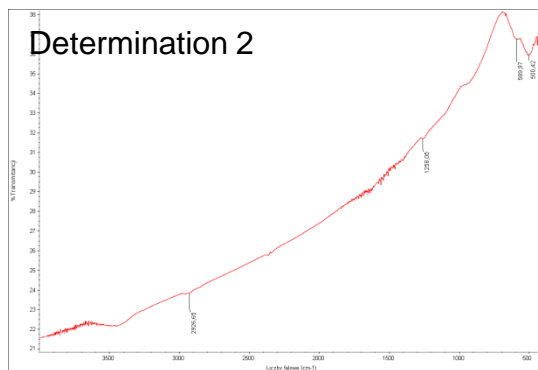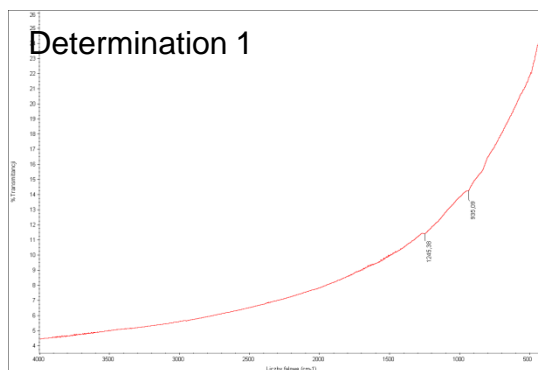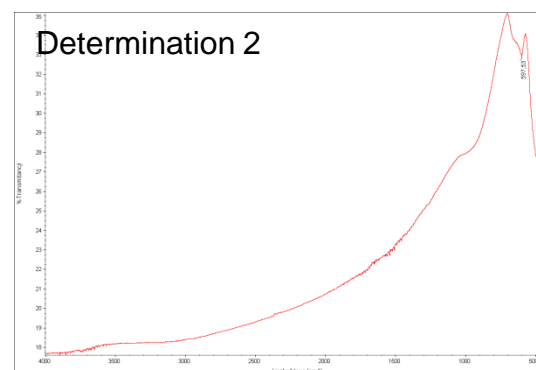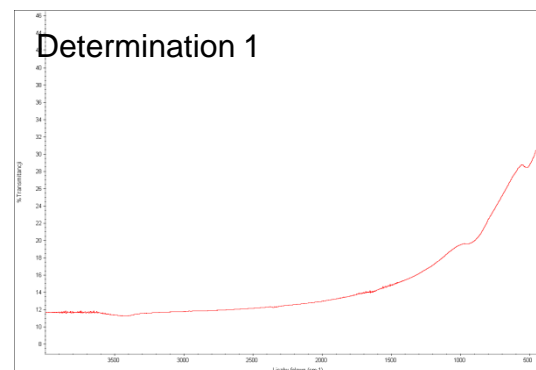
Apparently, there is no Mn-N stretch in the mid-infrared region.

Observed bands at <1000 cm^{-1} are due to Mn-O modes in oxidized products.

Results –
SEM/EDS examination

Powder, 500 ºC, 4 hrs

Higher N/O proportions
for higher pyrolysis temperatures

Powder, 900 ºC, 4 hrs

„Spongy" large particles
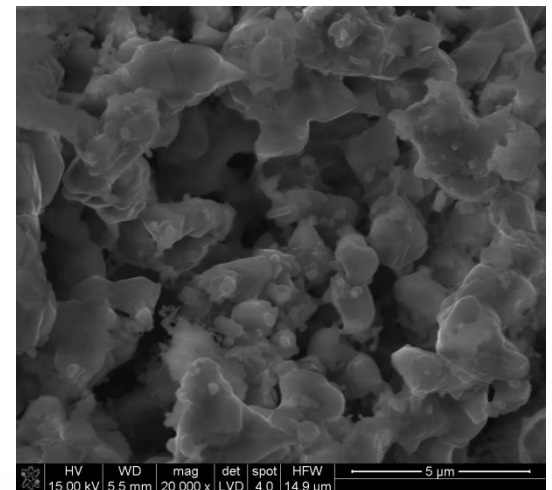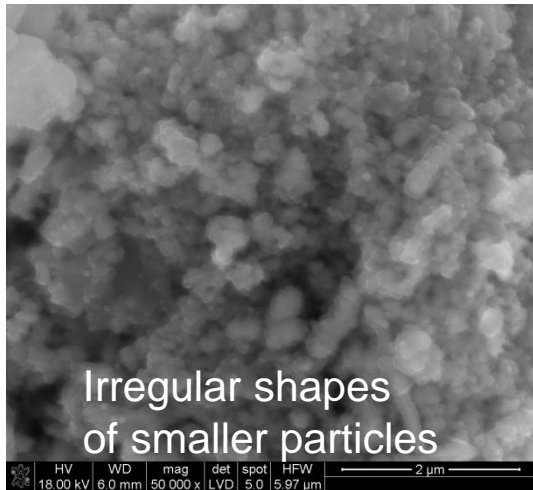
the same 5 μm scale bar
different crystallite sizes

Irregular shapes
of smaller particles

Particle shape is not, likely,
altered by surface oxidation

Conclusions

➢ <u>A new precursor system Mn[N(TMS)$_2$]$_2$ / NH$_3$ is shown to result</u> *via* transamination/deamination reactions in the rare nanocrystalline powders of manganese nitride.

➢ <u>Tetragonal η-Mn$_3$N$_2$ is the only polymorph obtained</u> in the pyrolysis range from 150 up to 900 ºC, the product from the latter temperature showing some changes in polymorphism.

➢ <u>The average crystallite size ranges from *ca.* 4 nm (pyrolyis at 150 ºC) to some +100 nm (pyrolysis at 900 ºC)</u> enabling a control of the nitride's crystallites in the nanosized region.

➢ Nanopowders of η-Mn$_3$N$_2$ are <u>extremely air-sensitive</u>.

Thank You For Your Attention